Radio Science, Volume 33, Number 4, Pages 929–939, July–August 1998

Influence of cloud temperature on brightness temperature and consequences for water retrieval

Ada Vittoria Bosisio[1] and Cécile Mallet

Centre d'études des Environnements Terrestre et Planétaire, Vélizy, France

Abstract. In this paper we show that to improve existing radiometric methods to estimate path-integrated cloud liquid water, the physical approximations commonly used concerning the direct model have to be reconsidered. In fact, even if the problem that consists in deducing the brightness temperatures from atmospheric quantities is rigorously solved (for a nonscattering atmosphere) by means of the radiative transfer equation, the relation between radiometric temperatures and one physical global quantity integrated content is not always determined from theoretical considerations. In all the dual-frequency retrieval models commonly used, the method always consists in the separation of the two water phases based on two radiometric measurements: one at a vapor-sensitive frequency and one at a cloud-sensitive frequency. The variations in the vertical absorption profile are neglected, in particular the temperature one, thus leading to linear expressions that allow an easier resolution of the inverse problem. Through an important set of simulated data, the authors have proved that a new global variable, which allows us to take the temperature profile into account, can greatly improve the modelization of the direct problem. The introduction of this quantity helped the authors to show that the relationship between brightness temperature and liquid water content is a nonlinear one. Even if the analytical inversion of the direct model allows only a relatively small improvement in water vapor and liquid water prediction, the consequences for the inverse problem are also discussed. To improve the existing dual-frequency algorithm, additional information sensitive to temperature profile is needed. For example, a third radiometer frequency can improve the inverse algorithm, but it should be used in a nonlinear expression.

1. Introduction

The use of ground-based radiometers for measuring the vertically integrated amounts of water vapor and cloud liquid is well established. The principles of dual-frequency measurement of liquid water and water vapor were first proposed by *Staelin* [1966] and carried on, in particular, by *Westwater* [1978]. Even if various algorithms are possible, the method always consists of the separation of the two water phases based on two radiometric measurements: one at a vapor-sensitive frequency and one at a cloud-sensitive frequency. Many authors have performed several tests to compare different dual-frequency retrieval methods. *Snider et al.* [1980] performed an experimental test, *Chong Wei et al.* [1989] assessed the accuracy of the different radiometric methods by simulations, and *Lavergnat et al.* [1993] compared several retrieval models in terms of statistics derived from measurements performed during the Olympus Propagation Experiment. If we consider the findings of these authors, we can conclude that all the retrieval methods studied give similar results except for the relatively high values of the integrated water content. In a more quantitative way, the conclusion is that whatever model is used, the overall rms error of liquid water retrieval is at least 30%. Concerning the water vapor retrieval, the smallest rms error is only 9%. However, for all methods, the biases and the rms deviations increase with increasing liquid amount. In all the dual-frequency retrieval models the variations in the vertical absorption profile are neglected, but nevertheless, the liquid water absorption profile, in particular, is very sensitive to temperature profile. As explained by *Westwater* [1978], one of the limiting factors in the determination of the water effect on radiometric measurements during cloudy conditions is the uncertainty related to cloud physical temperature.

[1] Now at Centre National d'Etudes des Télécommunications, Issy-les-Moulineaux, France.

Paper number 98RS00949.
0048-6604/98/98RS-00949$11.00

This suggests that the approximations commonly used concerning the direct model have to be reconsidered. As explained in the next section, neglecting vertical profile dependence and, in particular, the temperature one, leads to obtaining a linear expression relating integrated water content and atmospheric attenuations, which make the inversion problem easier.

Before studying the inverse problem, we propose here to improve the direct problem (often neglected) to select a new global variable that allows us to take the temperature profile into account. For this task a database of simulated data has been built up, and besides all quantities commonly implied, such as radiometric sky temperature T_{bf}, integrated liquid water content L, and water vapor content V, we added a new physical parameter. We have called it "liquid water temperature" T_L, and it corresponds to the mean physical temperature of clouds. In other words, we want to describe the radiometric sky temperature at frequency f with the following general expression:

$$T_{bf} = F_f(V, L, T_L) \tag{1}$$

2. Classical Approach

The physical basis is that the radiation incident upon a radiometer antenna is a frequency-dependent complex function of the vertical profiles of atmospheric temperature, pressure, water vapor, and liquid water density. We begin this part by reminding readers of the radiative transfer equation; then we present the approximations of the radiative transfer equation inherent in the dual-frequency linear inversion method commonly used.

For the frequency f, the sky brightness temperature observed at the ground surface, for a nonscattering atmosphere, is given by the equation of radiative transfer [*Chandrasekhar*, 1960]:

$$T_{bf} = T_c \exp[-\tau(f, \infty)] + \int_0^\infty T(z) \exp[-\tau(f, z)] k(f, z)\, dz \quad [\mathrm{K}] \tag{2}$$

where $k(f, z)$ and $T(z)$ are the atmospheric absorption coefficient at frequency f and the physical temperature at height z, respectively; T_c is the cosmic background temperature; and $\tau(f, z)$ is the optical depth given by

$$\tau(f, z) = \int_0^z k(f, y)\, dy \quad [\mathrm{Np}] \tag{3}$$

In the microwave range, between 10 and 60 GHz, atmospheric absorption is due to three contributions: oxygen (k_{O_2}), water vapor (k_v), and liquid cloud water (k_l). The total atmospheric attenuation, at a given microwave frequency, may therefore be expressed as the sum of the atmospheric attenuation due to water vapor (A_{fv}), oxygen (A_{fO_2}), and cloud liquid water (A_{fl}):

$$A_f = 4.343 \int_0^\infty (k_{O_2}(f,z) + k_v(f,z) + k_l(f,z))\, dz = A_{fO_2} + A_{fv} + A_{fl} \quad [\mathrm{dB}] \tag{4}$$

In order to perform the retrieval of integrated liquid water content L and water vapor content V by means of a dual-frequency radiometer, the following approximations are generally used. The radiative transfer equation (2) can also be written as

$$T_{bf} = T_c \exp[-\tau(f, \infty)] + T_{mf}\{1 - \exp[-\tau(f, \infty)]\} \quad [\mathrm{K}] \tag{5}$$

where the mean radiating temperature T_{mf} is a profile and frequency-dependent quantity:

$$T_{mf} = \frac{1}{\{1 - \exp[-\tau(f, \infty)]\}} \cdot \int_0^\infty T(z) \exp[-\tau(f,z)] k(f,z)\, dz \tag{6}$$

The total attenuation, in decibels, follows from

$$A_f = 4.343\tau(f, \infty) = 10 \times \log\left(\frac{T_{mf} - T_c}{T_{mf} - T_{bf}}\right) \tag{7}$$

For a given frequency in the considered band, the contribution of oxygen to the total attenuation is approximately constant [*Rosenkranz*, 1975].

Concerning the contribution of water, the mass absorption coefficient is often used to obtain a linear relation between the total attenuation of water vapor A_{fv} (correspondingly, liquid water A_{fl}) and the integrated water vapor content V (correspondingly, liquid content L) in kg m^{-2} or millimeters. The defining equation, for any profiles, of the mass absorption

coefficient for water vapor a_{fv} and liquid water a_{fl} are the following:

$$A_{fv} = 4.343 \int_0^\infty k_v(f, z)\, dz = a_{fv}V$$
$$A_{fl} = 4.343 \int_0^\infty k_l(f, z)\, dz = a_{fl}L \tag{8}$$

However, the mass absorption coefficients a_{fv} and a_{fl} depend on the vertical profiles of temperature, pressure, and water vapor or liquid water, respectively. On an ensemble of profiles, average mass absorption coefficients can be estimated.

For a dual-channel radiometer operating at two frequencies f_1 and f_2, the previous approximations lead to the following linear system:

$$A_{f_1} = A_{f_1O_2} + a_{f_1v}V + a_{f_1l}L$$
$$A_{f_2} = A_{f_2O_2} + a_{f_2v}V + a_{f_2l}L \tag{9}$$

This approach links the radiometric brightness temperature's values with the integrated content V and L in using the system (9) and the following expression deduced from (7), where T_{mf} is fixed:

$$T_{bf} = T_c \times \exp\left(-\frac{A_f}{4.343}\right) + T_{mf}\left[1 - \exp\left(-\frac{A_f}{4.343}\right)\right] \tag{10}$$

Then, the inversion of system (9) allows us to estimate the two quantities V and L from atmospheric total attenuation derived by radiometric measurements at two frequencies in using (7). The two frequencies f_1 and f_2 have to be chosen in such a way that the emitted radiation is particularly sensitive to water vapor at one of the frequencies and to cloud liquid water content at the other:

$$V = c_{0v} + c_{1v}A_{f_1} + c_{2v}A_{f_2}$$
$$L = c_{0l} + c_{1l}A_{f_1} + c_{2l}A_{f_2} \tag{11}$$

According to the considered inversion algorithm, different ways are employed to obtain the inversion coefficients c_{iv} and c_{il}. They may be determined by calculations from a mean atmosphere or from statistical linear regressions performed on simulated data.

This method implies that the effective atmospheric temperature T_{mf} is known. T_{mf} depends on the vertical atmospheric profiles, this variation being some 10 K, and leads to an uncertainty in the estimation of the water content. In the same way, the correctness of system (9) depends on the fact that coefficients A_{fO_2}, a_{fv}, and a_{fl} are considered independent of variations in the atmospheric profiles. These variations are yet relatively significant. Concerning liquid water, *Staelin*'s [1966] formula shows that the $k_l(f, z)$ absorption coefficient decreases by about 3% for a temperature increase of 1 K. Thus it should be considered that coefficient a_{fl} is not constant and has a minimum variability of about 25% [*Westwater and Guiraud*, 1980].

3. Simulated Data

To value the performance of the direct model that we propose here, we need brightness temperature values in order to compare predicted values with theoretical values. Such a comparison requires us to simultaneously measure radiometric sky temperature T_{bf} and the corresponding significant integrated parameter, i.e., V, L, and T_L (defined in section 4.1).

A great amount of multifrequency brightness temperature measurements are available for the microwave remote sensing community. Unfortunately, the scarcity of in situ meteorological data concerning cloud systems makes it necessary to tackle the problem through simulated data. In other words, we have selected an important set of representative atmospheric profiles to compare the brightness temperature estimated by means of the direct model (expression (1)) with those computed with the radiative transfer equation (2).

The atmospheric profiles are obtained starting from radio sounding measurements to which liquid water profile has been added (section 3.2). We have then used a propagation model to compute the absorption coefficients of water vapor k_v, liquid cloud water k_l, and oxygen k_{O_2}. For frequencies lower than 60 GHz, in clear-sky conditions or in the presence of clouds bearing droplets with radii sufficiently small (<100 μm), the scattering effect of clouds is negligible [*Ulaby et al.*, 1981].

3.1. Radio Soundings

A great number of radio sounding measurements have been considered to set up a database of atmospheric conditions as representative as possible. Data are collected during the Global Atmospheric Research Program (GARP) measurements campaign performed in 1979. Radiosondes were launched in

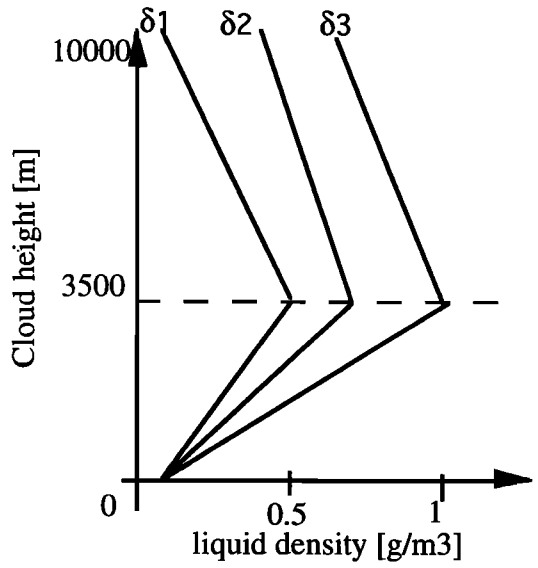

Figure 1. Liquid water density (g m^{-3}) as a function of cloud height.

site in both hemispheres twice a day, at midnight and at noon, and so represent a good description of a great number of possible atmospheric conditions from the seasonal and the geographical point of view. Each radio sounding profile in the GARP database contains the following quantities: pressure, temperature, and dew point temperature vertical profiles. Data, hour, latitude, longitude, and altitude are also included. In the framework of this study, we have not considered information concerning wind and cloud coverage, the former being more useful for meteorological studies and the latter being almost qualitative. Vertical radio sounding profiles have been quality checked, and those with maximum height less that 5 km have been eliminated.

3.2. Cloud Model

Standard radio sounding measurements, as is well known, do not include measurement of the liquid water density in the atmosphere. As a consequence, it is necessary to use a model to describe its contribution to atmospheric absorption. At first, such a model has to decide about the presence of a cloud, if any, and then to give the liquid water density profile inside it. To assess if a cloud is present or not, an approach well appreciated by other authors has been chosen: A cloud is present if the value of the relative humidity (RH) is greater than 95%. According to this, to each "cloudy" radio sounding profile, that is, to each profile in which the relative humidity is greater than 95%, the liquid water density information has been added. Cloud thickness is then defined by the two height values at which RH = 95%.

Concerning the liquid water density profile inside the cloud, a new model has been defined. In this model, as in most of the existing ones [*Salonen and Uppala*, 1991; *Decker et al.*, 1978], the liquid water density is constant in the cloud; nevertheless, it is designed to take atmospheric profile dependence into account.

To do this, we have first defined a bilinear vertical profile of the liquid water density (see Figure 1). In fact, according to *Slobin* [1982], its value depends on the height of the cloud, since cloud structure is a function of its location in the sky. The linear behavior has been chosen on the basis of information deduced from meteorological considerations. Lowest values (height equal to zero) and highest values (at 3500 m) for liquid water density have been chosen according to Slobin's classification.

In addition, clouds at the same height may bear different amounts of liquid water, so a unique choice does not take into account all the possible variations, since it inevitably describes an average situation. Climatological or seasonal factors have a significant influence on cloud type and distribution [*Salonen et al.*, 1990]. To describe all possible atmospheric conditions, three vertical profiles have been defined. To obtain a variability in liquid content simulations, we defined for each "wet" radio sounding profile three atmospheric profiles; that is, three different liquid water densities have been chosen for each cloud.

The constant value inside the cloud is then given by the following expression:

$$\delta_i = \frac{\delta_i(\text{top}) + \delta_i(\text{bottom})}{2} \qquad i = 1, 2, 3 \qquad (12)$$

in which, liquid density δ_i (top) and δ_i (bottom) are read in Figure 1 for the height of the top and the height of the bottom of the cloud. To verify that the values given by the proposed model properly represented the typical values of liquid water integrated content, we have compared a histogram of simulated L values derived by our database with others present in the literature.

3.3. Atmospheric Database

Information deduced by radio sounding or defined by cloud model has been used to compute some

integral quantities of interest, water vapor content V and liquid water content L, by integration of a given vertical profile. Atmospheric profiles have also been used to compute brightness temperature T_{bf} and atmospheric attenuation A_f at zenith pointing at 27 frequencies, between 10 and 90 GHz (chosen among those dedicated to the passive space research) by means of *Liebe et al.*'s [1993] MPM93 model. Each selected profile gives rise to a synthetic atmosphere, that is, a specific sky condition described by parameters in Table 1.

The database so derived from the 110,511 radio soundings contains up to 149,588 synthetic atmospheres, 89,503 in clear-sky conditions and 60,085 in cloudy ones. Moreover, a reduced database has been defined, the so-called European selection, since it collects all measurements relative to location with latitude between 39° and 60° and longitude between −10° and 25°. These data are divided into two sets: the first set is used for training, and the second set is used for testing. Table 2 shows the number of atmospheres contained in each of the two sets. The use of this simulated database consisting of radiometric quantities and significant geophysical parameters computed on synthetic atmospheric profiles will allow us to simplify the complex atmospheric transfer function of the atmosphere.

Table 1. Information Associated With Each Synthetic Atmosphere

Parameter	Unit
Geographical coordinates	
altitude above sea level	m
atmospheric pressure at ground	Pa
temperature at ground level	°C
relative humidity at ground level	%
Atmospheric integral quantities	
cloud number	[−]
liquid water temperature T_L (see section 4.1)	°C
water vapor integrated content V	kg m^{-2}
liquid water integrated content L	mm
Radiative transfer calculations	
brightness temperature T_{bf} at 27 frequencies, between 10 and 90 GHz	K
atmospheric attenuation A_f at 27 frequencies, between 10 and 90 GHz	dB

Table 2. Distribution of Atmospheres in the Different Subsets

	Training Set		Test Set	
	Clear	Cloudy	Clear	Cloudy
European selection	5,808	5,546	6,440	5,622
Worldwide	43,225	29,072	46,278	31,013

4. Direct Model

The direct problem, which consists of deducing the brightness temperatures from atmospheric quantities, is rigorously solved by means of the radiative transfer equation (2) and of the *Liebe et al.* [1993] microwave propagation model. This section deals with a different way to approach the direct problem (equation (1)) consisting, namely, of the modelization of the radiative transfer equation, since the relation between radiometric temperatures and one given physical global quantity is not always determined from theoretical considerations. For example, for the frequency channel around 22 GHz the radiometric temperature is very sensitive to water vapor. However, even if the radiometric temperature depends on the vertical profile of water vapor partial pressure, the quantity to be estimated is the water vapor integrated content V. The liquid water content L also has a great influence on radiometric temperature; however, this influence depends on the physical temperature of the cloud layer. That is why it is of prime importance to select the significant geophysical parameters.

As explained in section 2.2, the classical approach concerning the direct model (equations (9) and (10)) consists of taking only V and L into account and neglecting the temperature profile dependence (if T_{mf} is fixed). The aim of this section is to test if the direct model can be improved in adding a new global variable T_L.

In other words, before studying the inverse problem, it is very important to make clear these questions: Is the influence of cloud temperature variability a negligible effect? If not, can it be taken into account? Which global parameter is able to take this influence into account?

4.1. Liquid Water Temperature T_L

Cloud height has a relevant effect on brightness temperature. We can, in fact, show that for the same L value we obtain different brightness temperature values, depending on cloud location in the sky.

To show this, we have performed a simple but clarifying simulation. Temperature, pressure, and vapor density profile have been chosen according to the U.S. standard atmosphere [*Cole et al.*, 1968]. Concerning the liquid water profile, we have considered a cloud with an integrated content L equal to 0.5 mm

and a thickness Δh equal to 500 m. We have thus chosen to locate the same cloud at two different positions: the first at low height (starting at ground level) and the second at a higher height (bottom of the cloud at some 6000 m). We obtain differences in the corresponding calculated brightness temperatures equal to 13 K at 23.8 GHz and 20 K at 31.7 GHz. The relation between atmospheric attenuation and brightness temperature (equation (7)) leads to differences in attenuation values equal to 0.25 dB at 23.8 GHz and 0.38 dB at 31.7 GHz for the two positions of the cloud. In using the classical approach (equation (11)), with inversion coefficients c_{ij} determined from statistical linear regressions performed on the simulated database, we deduce two different values for the integrated contents V and L. The two clouds (same V, same L, and height difference of 6000 m) lead to variations of 20% in the retrieved water vapor content V and of 70% in the retrieved liquid water integrated content L.

These results evidence the need of a new global quantity to improve the direct model. This quantity has to bring information on the atmospheric profile in the cloud layer. We have thus tried to improve the direct model in adding the following parameter, called liquid water temperature T_L:

$$T_L = \frac{\int_{h_1}^{h_2} T(z)\delta_i \, dz}{L} \tag{13}$$

where $T(z)$ is the temperature profile, δ_i is liquid water density, and h_1 and h_2 are cloud bottom and top heights.

For a better estimation of the contribution of water in each physical status, that is, the vapor or liquid one, we have modeled the contribution of each one separately. We have called T_{bf}^V the water vapor contribution and T_{bf}^L the liquid water contribution to the brightness temperature values. If we consider clear-sky conditions, $T_{bf} = T_{bf}^V$, we can find the relation between water vapor and brightness temperature. In cloudy conditions we can then subtract the water vapor contribution T_{bf}^V to study the liquid water dependence.

The database has then be divided into two subsets: one collecting all clear-sky atmospheres (that is, $L = 0$) and the other collecting cloudy ones. Starting from these two subsets, we have defined a new expression of brightness temperature as a function of the integral quantities V, L, and T_L.

4.2. Clear-Sky Analysis

Clear-sky analysis aims to relate the absorption contribution of water vapor to brightness temperature values. When clear sky occurs, only atmospheric gases are present. Here we consider only the contribution due to water vapor and oxygen, since the effect of the other gases is negligible. Water vapor density, and so its integrated content, vary both in space and time, while oxygen concentration is practically constant.

For frequencies lower than 45 GHz we can consider the water vapor contribution V as the only unknown quantity, taking the oxygen contribution as a constant factor. Simulation results let us argue that in clear-sky conditions, there is a strong linear relation between brightness temperature and V:

$$T_{bf} = T_{bf}^V = m_1 \times V + m_2 \qquad f < 45 \text{ GHz} \tag{14}$$

To characterize the clear-sky behavior frequencies higher than 45 GHz, we have to add the oxygen contribution; this can be done with a linear relation between brightness temperature and the pressure at ground level P_0. Pressure has been introduced since we consider sites located at different height above sea level, and this introduces a bias in brightness temperature estimation, particularly above 45 GHz, where the oxygen contribution has an important influence.

$$T_{bf} = T_{bf}^V = m_1 \times V + m_2 + m_6 \times P_0 \qquad f > 45 \text{ GHz} \tag{15}$$

The values of the coefficients m_i and corresponding algorithm errors are presented in section 4.4.

4.3. Cloudy-Sky Analysis

The assessment of an analytical expression that takes into account cloud contribution to brightness temperature values presents more difficulties if compared with the situation in which the sky is clear. While water vapor contribution has a linear weight (equations (14) and (15)), this is not the case for liquid water content. Our first task is thus to obtain the shape of the relation between the brightness temperature and the liquid water content, taking the new global variable T_L into account. To reduce noisy effects and knowing the contribution due to the water vapor presence, we have at first focused our attention on a derived unknown, that is, brightness temperature subtracted from the clear-sky contribution:

$$T_{bf}^L = T_{bf} - T_{bf}^V \tag{16}$$

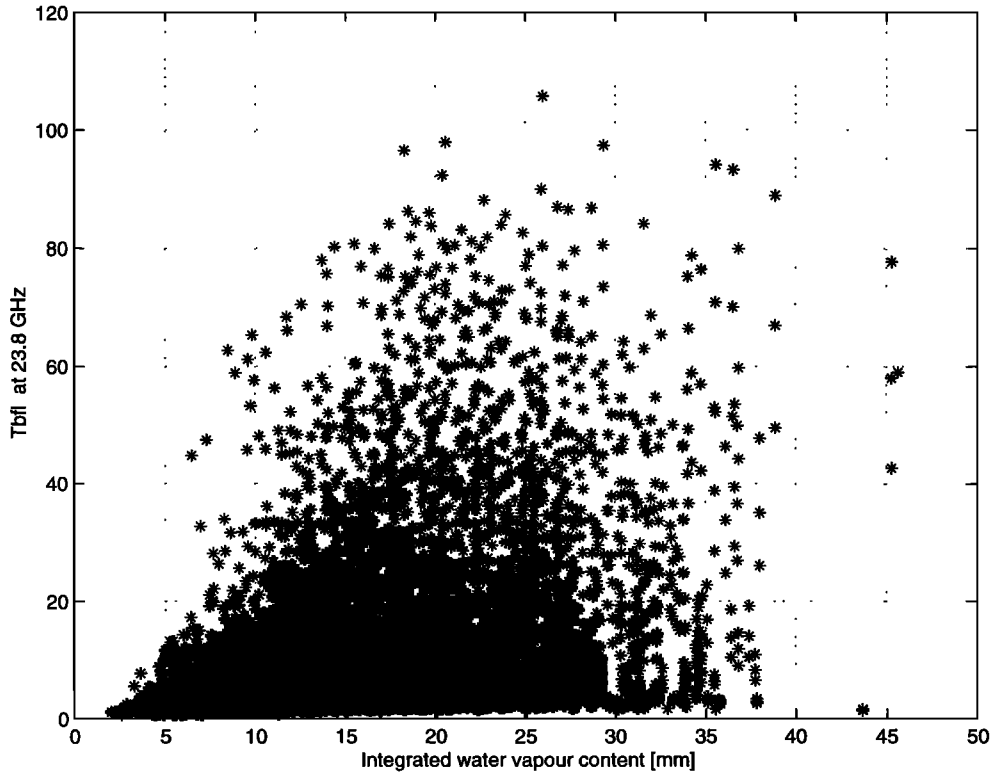

Figure 2. Cloudy contribution to brightness temperature at 23.8 GHz as a function of integrated water vapor content.

where T_{bf}^{V} takes the water vapor contribution into account as stated in (14) or (15) and T_{bf}^{L} is the "cloudy" contribution to the brightness temperature value. Theoretically, optical depth for water vapor can be subtracted from the overall value, giving the liquid optical depth. This is not true for brightness temperatures. In fact, the water vapor contribution to brightness temperature is not exactly the same whether clouds are present or not. However, as shown in Figure 2, the liquid water brightness temperature T_{bf}^{L} appears to be independent of the integrated water vapor content. This justifies the use of this quantity to study the liquid water dependence. In fact, this abstraction is useful to find the shape of the analytical expression of the direct model.

The T_L parameter (equation (13)) plays an important role, since it takes into account both liquid water density inside the cloud and temperature vertical profiles. According to this and to find out the shape of the function we are looking for, we have divided our cloudy synthetic atmospheres database into seven classes, having chosen T_L values ($-10° < T_L <$ $+25°$C) as criteria. T_L parameterization has led to a narrower shape of scatter diagrams reported in Figure 3 that justify the choice of T_L as a meaningful parameter in detecting liquid water contribution. In fact, a preliminary analysis on these plots has suggested for the fitting function an exponential shape. The proposed shape for T_{bf}^{L} is the following:

$$T_{bf}^{L} = m_3[1 - \exp(-m_4 T_L L - m_5 L)], \quad (17)$$

valid for each frequency f considered in the database.

4.4. Comparisons and Results

Starting from these considerations, the direct expression for the estimated brightness temperature is

$$\hat{T}_{bf} = m_1 V + m_2 + m_3(1 - \exp(-m_4 T_L L - m_5 L)) + m_6 P_0 \quad (18)$$

with m_6 equal to zero if f is lower than 45 GHz and the m_i coefficient obtained by means of a nonlinear regression. Most nonlinear least squares methods

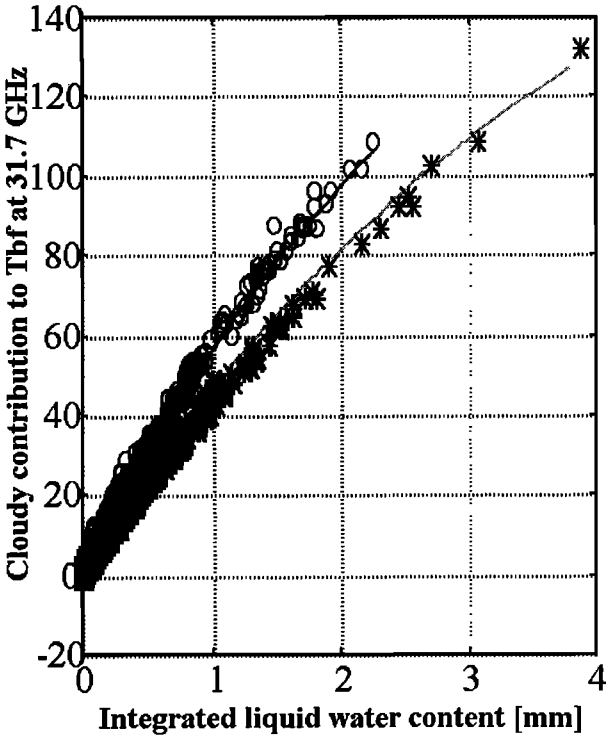

Figure 3. Sensitivity of T_b^L to liquid water temperature T_L: circles indicate $-5° < T_L < 0°C$, and asterisks indicate $5° < T_L < 10°C$.

require large amounts of iterative calculations and a good initial guess for a satisfactory estimate of the coefficients. Among the methods available, we have chosen Levemberg-Marquadt [*Press et al.*, 1989], as recommended in the literature [*Comincioli*, 1990]. The initial values for m_i coefficients are those obtained separately as stated in sections 4.2 and 4.3. Table 3 presents the final results, computed on the training set for the whole database and for the European selection.

The comparison of this new direct model (equation (18)) with the classical approach (equations (9) and (10)) is performed at frequencies of 23.8 and 31.65 GHz. Table 4 compares the following four parameters: the rms error of the regression, often used to characterize algorithm quality; the upper decile (U.D.) of the error of the regression, that is, the error corresponding to the cumulative distribution function equal to 0.9; and the regression slope p and the intercept q as derived by a linear regression between simulated temperature T_{bf} and estimated temperature $\hat{T}_{bf}$.

The two values that appear for each parameter in Table 4 correspond to the values computed on the training set and on the test set (training/test). Results are here again presented for the whole database and for the European selection. All the parameters are also computed for the classical algorithm to allow comparison.

If we consider the whole database, where a very wide variety of different atmospheric conditions are presented, the three global parameters V, L, and T_L allow an estimation of the brightness temperature with an error lower than 1.5 K at 23.8 GHz and lower than 2.6 K at 31.7 GHz for 90% of the cases. If only V and L are taken into account, the error is less than 4.8 K for the two frequencies. These results evidence the improvement obtained considering further information related to temperature vertical profile T_L; in particular, the addition of this global parameter T_L in the direct model allows a modeling of the brightness temperature at 23.8 and 31.7 GHz that is three and two times better, respectively, than the classical one.

5. Consequences for the Inverse Model and Conclusions

5.1. A Three-Frequency Nonlinear Inverse Model

The results obtained by solving the direct problem have been interpreted to build up an algorithm

Table 3. Coefficients Relative to the Entire Database and Relative to the European Selection

	$m1$, K mm^{-1}	$m2$, K	$m3$, K	$m4$, K^{-1} mm^{-1}	$m5$, mm^{-1}	$m6$, K Pa^{-1}
			Whole Database			
23.8 GHz	1.3858	7.5248	158.7898	−0.0067	0.2012	0
31.65 GHz	0.5932	8.7713	210.6996	−0.0064	0.2752	0
			European Selection			
23.8 GHz	1.4316	7.033	167.0279	−0.0061	0.1896	0
31.65 GHz	0.5806	9.3245	214.6364	−0.0064	0.2681	0

Table 4. Results and Comparisons Relative to the Entire Database and Relative to the European Selection

	Linear Algorithm				Present Study			
	rms	UD	p	q	rms	UD	p	q
				Whole Database				
23.8 GHz	2.7/2.6	5/4.8	0.94/0.94	0.61/0.86	1.12/1.1	1.5/1.4	1.0/0.99	0.08/0.16
31.65 GHz	3/2.9	4.9/4.8	0.97/0.95	−0.1/0.34	1.6/1.6	2.6/2.6	1.0/0.99	0.12/0.16
				European Selection				
23.8 GHz	1.8/1.9	2.8/3	0.98/0.96	−0.11/0.14	0.71/0.71	0.93/1.0	1.0/1.0	0.04/0.01
31.65 GHz	2.2/2.3	3.3/3.4	0.99/0.98	−0.31/−0.13	1.17/1.24	1.76/1.81	1.0/0.99	0.07/0.14

First value is from the training set, and second value is from the test set. UD, upper decile.

leading to the retrieval of water vapor V and liquid water integrated content L. The goal of the inverse problem is to predict these two quantities, starting from known brightness temperature values. Application of such an algorithm may be foreseen for V and L retrieval at an unattended ground-based radiometer.

Resolution of the direct problem points out two consequences relative to inverse problem. The first is the need of adding information concerning cloud temperature. This point was previously emphasized by *Westwater* [1978] and *Han and Thomson* [1994]. A recent paper by *Han and Westwater* [1995] shows how soundings from a radio acoustic sounding system and a cloud ceilometer can be incorporated to improved inversion of brightness temperatures. The second consequence is that if only radiometric measurements are allowed, the need of a nonlinear approach is also emphasized. In fact, the necessity of adding a third global parameter T_L in the direct model implies the addition of a third brightness temperature at a different frequency in the inverse model. Subsequently, we have to study the improvement of an inverse model obtained in using a three-frequency radiometer.

If we consider (18), we can observe that the relation between the liquid water integrated content L and brightness temperatures has been suggested to be nonlinear. These conclusions confirm a result obtained by *Mallet and Lavergnat* [1992], who showed that the use of a third frequency in a linear retrieval algorithm does not lead to any improvement.

A new inverse model can thus be obtained by inversion of the following system, where F_i is the function given in (18) and the index ($i = 1, 2, 3$) corresponds to three different frequencies:

$$\begin{aligned} T_{bf_1} &= F_{f_1}(V, L, T_L) \\ T_{bf_2} &= F_{f_2}(V, L, T_L) \\ T_{bf_3} &= F_{f_3}(V, L, T_L) \end{aligned} \tag{19}$$

The choice of the three selected frequencies has been driven by the need to have two frequencies sensitive to water presence (classical values have been chosen) in the 20- to 30-GHz band [*Westwater*, 1978; *Hogg et al.*, 1983; *Westwater et al.*, 1990] and of one sensitive to the vertical profile of temperature [*Schiavon et al.*, 1993; *Basili et al.*, 1994]. Frequencies chosen are 23.8, 31.65, and 50.2 GHz.

The inverse model obtained in an analytical way by inversion of the direct model (equation (19)) allows a relatively small improvement. Concerning the retrieval of the water vapor integrated content V, if we compare the error obtained with the one obtained with the classical approach (equations (7) and (11)), the rms error as well as the upper decile are divided by 1.5. That is, we obtain an algorithm that supplies V with an error lower than 2 kg m^{-2} in 90% of the cases (the upper decile is lower than 1 kg m^{-2} if we consider only the European selection). Concerning the retrieval of the liquid water integrated content L, the new inverse model allows an improvement of 0.01 kg m^{-2} compared with the classical approach. That is, we obtain an algorithm that supplies L with an error lower than 0.07 kg m^{-2} in 90% of the cases (the upper decile is lower than 0.05 kg m^{-2} if we consider only the European selection).

6. Conclusion

Concerning the direct problem, we have obtained a great improvement in the brightness temperature

estimation with the addition of a third global parameter T_L that brings information on the cloud temperature. Satisfactory results are also obtained for the inverse model. In the first case, introduction of T_L has improved the prediction in estimation of brightness temperature value at each of the chosen frequencies. This confirms that for a good estimation it is necessary to take into account vertical structure of the atmosphere and that a lack of knowledge about cloud height in the sky may introduce errors of some tens of kelvins. Moreover, nonlinearity of the relationship between brightness temperature and global parameters V and L has been proved.

As a conclusion we can argue that the resolution of the inverse problem with success has to be refined. After this study of the direct model we come to the conclusion that even if the analytical inversion allows a relatively small improvement, a future study consisting of research of a nonlinear three-frequencies algorithm will certainly improve the retrieval of V and L. The use of a neural network model, for example, will present the advantage that it is not necessary to determine the form of the inverse model in advance.

References

Basili, P., P. Ciotti, and E. Fionda, Comparison of algorithms for the retrieval of water vapor, cloud liquid and atmospheric attenuation by microwave radiometry, in *Proceedings of PIERS 94*, Eur. Space Agency, Noordwijk, Netherlands, July 1994.

Chandrasekhar, S., *Radiative Transfer*, Dover, Mineola, N. Y., 1960.

Chong Wei, H. G. Leighton, and R. R. Rogers, A comparison of several radiometric methods of deducing path-integrated cloud liquid water, *J. Atmos. Oceanic Technol.*, *6*(6), 1001–1012, 1989.

Cole, A. E., A. Court, and A. J. Kantor, Model atmospheres, in *Handbook of Geophysics and Space Environment*, edited by S. L. Valley, chap. 2, U.S. Air Force Cambridge Res. Lab., Cambridge, Mass., 1968.

Comincioli, V., *Analisi Numerica: Metodi, Modelli, Applicazioni*, McGraw-Hill, New York, 1990.

Decker, M. T., E. R. Westwater, and F. O. Giraud, Experimental evaluation of ground-based microwave radiometric sensing of atmospheric temperature and water vapor profile, *J. Appl. Meteorol.*, *16*, 1788–1795, 1978.

Han, Y., and D. W. Thomson, Multichannel microwave radiometric observation at Saipan during 1990 tropical cyclone motion experiment, *J. Atmos. Oceanic Technol.*, *11*, 110–121, 1994.

Han, Y., and E. R. Westwater, Remote sensing of tropospheric water vapor and cloud liquid water by integrated ground-based sensors, *J. Atmos. Oceanic Technol.*, *12*, 1050–1059, 1995.

Hogg, D. C., F. O. Guiraud, J. B. Snider, M. T. Decker, and E. R. Westwater, A steerable dual-channel microwave radiometer for measurement of water vapor and liquid in the troposphere, *J. Clim. Appl. Meteorol.*, *22*, 789–806, 1983.

Lavergnat, J., P. Golé, and C. Mallet, Retrieval of atmospheric water from ground-based radiometry, in *Proceedings of an International Conference Concerning Programme Results, WPP-60 ESA*, pp. 595–602, Euro. Space Agency, Noordwijk, Netherlands, 1993.

Liebe, H. J., G. A. Hufford, and M. G. Cotton, Propagation modelling of moist air and suspended water/ice particles at frequencies below 1000 GHz, in *AGARD 52nd Specialist's Meeting of EM Wave Propagation Panel*, pp. 3-1–3-10, Advis. Group for Aerosp. Res. and Dev., Brussels, Belgium, 1993.

Mallet, C., and J. Lavergnat, Beacon calibration with a multifrequency radiometer, *Radio Sci.*, *27*(5), 661–680, 1992.

Press, W. H., B. P. Flannery, S. A. Teukolsky, and W. T. Vetterling, *Numerical Recipes in C*, Cambridge Univ. Press, New York, 1989.

Rosenkranz, P. W., Shape of 5 mm oxygen band in the atmosphere, *IEEE Trans. Antennas Propag., AP-23*, 498–506, 1975.

Salonen, E., and S. Uppala, New prediction method of cloud attenuation, *Electron. Lett.*, *27*(12), 1106–1108, 1991.

Salonen, E., S. Karhu, P. Jokela, W. Zhang, S. Uppala, H. Aulamo, and S. Sarkkula, Study of propagation phenomena for low availabilities, final report for European Space Agency, *ESTEC Contr. 8025/88/NL/PR*, Eur. Space Agency, Noordwijk, Netherlands, 1990.

Schiavon, G., D. Solimini, and E. R. Westwater, Performance analysis of a multifrequency radiometer for predicting atmospheric propagation parameters, *Radio Sci.*, *28*(1), 63–76, 1993.

Slobin, S. D., Microwave noise temperature and attenuation of clouds: Statistics of these effects at various sites in the United States, Alaska, and Hawaii, *Radio Sci.*, *17*(6), 1443–1454, 1982.

Snider, J. B., F. O. Guiraud, and D. C. Hogg, Comparison of cloud liquid content measured by two independent ground-based systems, *J. Appl. Meteorol.*, *19*, 577–579, 1980.

Staelin, D. H., Measurements and interpretation of the microwave spectrum of the terrestrial atmosphere near 1-centimeter wavelength, *J. Geophys. Res.*, *71*, 2875–2881, 1966.

Ulaby, F. T., R. K. Moore, and A. K. Fung, *Microwave Remote Sensing Active and Passive*, vol. 1, pp. 288–302, Addison-Wesley, Reading, Mass., 1981.

Westwater, E. R., The accuracy of water vapor and cloud

liquid determination by dual-frequency ground-based microwave radiometry, *Radio Sci.*, *13*(4), 677–685, 1978.

Westwater, E. R., and F. O. Guiraud, Ground-based microwave radiometric retrieval of precipitable water vapor in the presence of clouds with high liquid content, *Radio Sci.*, *15*, 947–957, 1980.

Westwater, E. R., J. B. Snider, and M. J. Falls, Ground-based radiometric observations of atmospheric emission and attenuation at 20.6, 31.65, and 90 GHz: A comparison of measurements and theory, *IEEE Trans. Antennas Propag.*, *38*(10), 1569–1579, 1990.

A. V. Bosisio, France Telecom, Centre National d'Etudes des Télécommunications, DMR/RMC, 38–40 Rue de General Leclerc, 92794 Issy-les-Moulineaux, Cedex 9, France. (e-mail: adavittoria.bosisio@cnet.francetelecom.fr)

C. Mallet, Centre d'études des Environnements Terrestre et Planetaire, 10–12, Avenue de l'Europe, 78140 Vélizy, France. (e-mail: bosisio@cetp.ipsl.fr; mallet@cetp.ipsl.fr)

(Received February 24, 1997; revised November 18, 1997; accepted March 20, 1998.)